Biostatistics and Biometrics
Open Access Journal
ISSN: 2573-2633

Research Article
Volume 11 Issue 2 - May 2023
DOI: 10.19080/BBOAJ.2023.11.555810

Biostat Biom Open Access J

Physicochemical Transformation Effect on the Relaxivity Enhancement of Iron Oxide Nanoparticles in Nuclear Medicine and MRI Imaging

Homeira Faridnejad*

Department of Physics, East Carolina University, Howell Science Complex, Greenville, NC 27858, United States

Submission: March 17, 2023; **Published:** May 11, 2023

***Corresponding author:** Homeira Faridnejad, Department of Physics, East Carolina University, Howell Science Complex, Greenville, NC 27858, United States

Abstract

Iron Oxide Nanoparticles (IONPs), one of the contrast agents for MRI scanners, will be designed to have high relaxivity since they have distinct physical properties attributed to the quantum size effect. There are several techniques for synthesizing IONPs also for Superparamagnetic iron oxide nanoparticles (SPIONs) and Ultrasmall Superparamagnetic iron oxide nanoparticles (USPIONs) by using some physicochemical transformation effects which can affect relatxivity time by controlling the size and surface which is used respectively as a T_2 contrast agent and T_1 or T_2 contrast agent. Biomedical imaging like computed tomography (CT), positron emission tomography (PET), and single-photon emission computerized tomography (SPECT). Magnetite (Fe_3O_4) and maghemite (γ-Fe_2O_3) are both single crystalline structures. Nanoparticles that are non-spherical such as octopus's cubes and rods have more than their spherical counterparts. Size and shape must be controlled because they determine the phase, crystallization, size, and magnetism of the contrast agent of MR-CT are called GION gold oxide particles as a dual contrast. It can be provided from uneven structural nanocomposites of radiolabeled and MNP-labeled essential materials, while the intensity of contrast in the tumor area increases over time, indicating that FAuNC@Fe_3O_4 is highly absorbed in the tumor. Radioactive elements that bind to IONP can be used in multimodal imaging and radiotherapy. The ^{99m}Tc -labeled NOTA-IONPs were fabricated as shell microbeads and DTPA-IONPs to observe the clearance and distribution of nanoparticles in vivo (Figure 1).

Keywords: Magnetic Resonance Imaging; IONPs; Relaxivity; SPIONPs; T_1 or T_2 Contrast Agent; USPIONPs; MR-CT; ^{99m}Tc-labeled; Biomedical Imaging

Introduction

Nowadays a huge number of people are suffering from cancer, so, this is a principle to find new methods to overcome this problem. Magnetic resonance imaging (MRI) is a commonly used tool for patient diagnostics, and it has several advantages a non-invasive procedure that does not require ionizing radiation and can provide high resolution of anatomical features [2-4] but it has some weaknesses like low sensitivity. MRI relies on contrast agents (CA) to enhance the visualization and better diagnose diseases, especially cancer cells [5,6]. CA in MRI imaging by changing the relaxation rate of surrounding hydrogen protons can provide us the desirable imaging with high magnetic relaxivity because it influences the positive and negative contrast of an image [7-9]. We have a wide variety of CAs, but among them are Iron oxide nanoparticles (IONPs), which are extensively used throughout biomedical [10-13]. More recently, an increasing interest in IONPs-based CAs has resurfaced not only for diagnostic purposes but also for therapy in the clinic. IONPs have physicochemical properties which are desired for medical imaging like MRI, Single photon emitted tomography (SPECT), positron emission tomography (PET), and Computed tomography (CT). because each one of the medical imaging scanners uses a contrast agent in MRI, and CT, and we can use radio pharmacy in nuclear medicine imaging like PET and SPECT. The extraordinary properties of IONPs, help us to label this with different materials. These properties are sphere Diffusion Model, size, and shape. Consequently, based on these properties we can use these IONPs in CA and radio pharmacies to enhance the signal and sensitivities of medical imaging, in the end, the diagnosis of diseases especially cancer will be enhanced.

In recent years, MRI signal has enhanced thanks to scientific advancements and increased focus on the physicochemical properties of IONPs [7,8]. It has generally been proven that the physicochemical properties of IONPs such as structure, size, shape,

and surface modification can affect the Relaxivity Enhancement in MRI [3,9]. In fact, by using the controlled synthesis of the size, shape, and structure of IONPs and their magnetic application in MRI, we can increase the MRI signal for diagnosing diseases and drug redelivery 64. In the past decades, a lot of attention has been paid to IONPs production in different shapes and sizes. Among them, temperature and pressure play a very crucial role in particle size and morphology of it, and these factors can be implemented by controlling its shape, size, and structure [14,15]. The results of this study showed that after 24 hours of incubation of cells and nanoparticles, more than 90% of the cells survived, which indicated that these nanoparticles did not have any dangerous effect on human health. As mentioned in previous paragraphs, another important parameter to enhance the MRI signal is increasing the relaxivity time [16]. By using IONPs as a CA, relaxivity time can be changed, since it is related to the size and composition of particles [2,12,17]. Relaxation time can also be determined by temperature and field in intensity or instance, it was reported that the use of a 22nm cube-shaped nanoparticles rate with a very high r^2 relaxivity at 761 mM^{-1} s^{-1} shows the tumor more clearly.

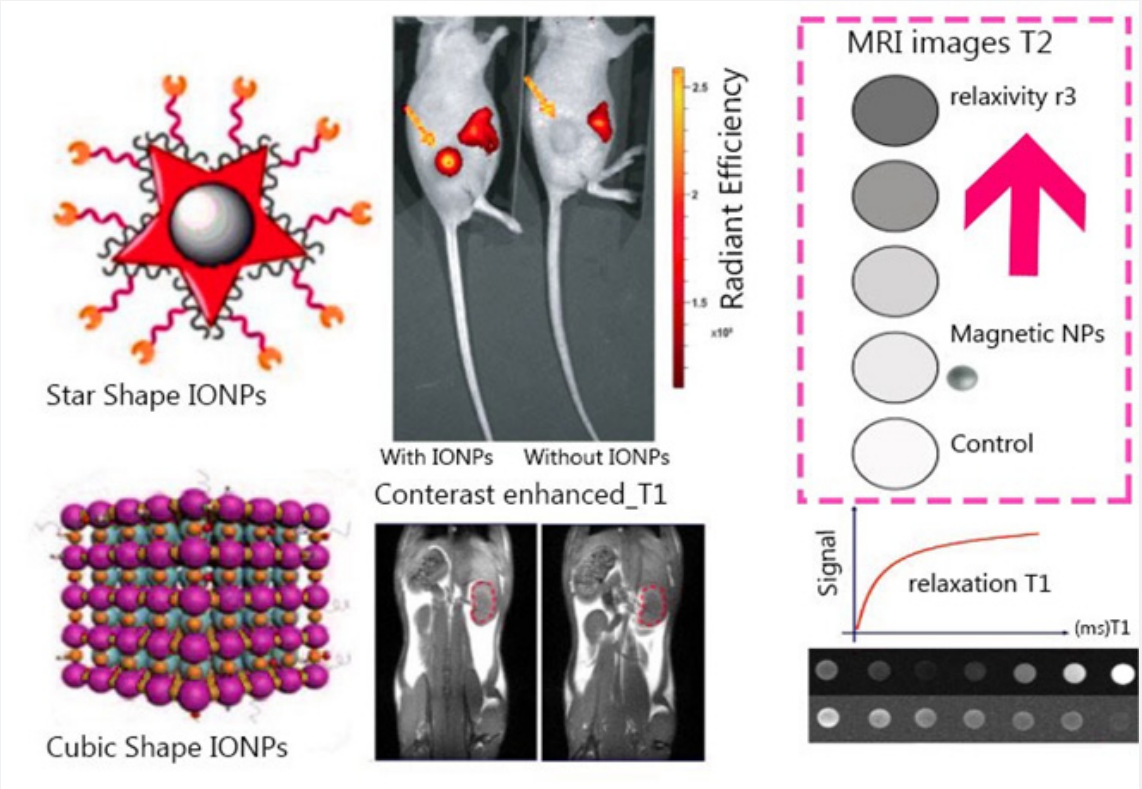

Figure 1: Radioactive elements that bind to IONP.

In this review paper, we discuss in detail the physicochemical transformation effect on the relaxivity enhancement of iron oxide nanoparticles, MRI signal, and relaxivity times. We also investigate Magnetic Resonance-Computer Tomography (MR-CT) bimodal imaging as well as radiolabeled iron oxide nanoparticles with radioisotope in medical imaging techniques, and how this multi-modular imaging radiolabeled with IONPs can enhance image sensitivities and resolutions. The growth of medical imaging technology has provided early detection of diseases [18-20]. The imaging methods, including positron emission tomography (PET), single-photon emission tomography (SPECT), MRI, and computed tomography (CT), have their strengths and weaknesses [21,22]. To overcome the disadvantages of each imaging technique, we can use multimodal imaging methods such as MR-CT, PET-CT and PET-MRI.

Physicochemical transformation effect on the MRI signal

A wide variety of attempts in manipulating the structural characteristics of IONPs is one of the big interesting to enhance their magnetic relaxivity and MRI signal. [23]. Because IONPs have potential applications in a variety of research fields. Physicochemical characteristics of IONPs including surface modification, size, shape, and crystal structure, led to a great deal of research to enhance MRI signal [24]. Besides the interesting properties of IONPs, they can shorten the relaxation time of protons and enhance the MRI signal [25]. These nanoparticles (IONPs) can generate a local magnetic field and they change the nuclear relaxation of magnetic nuclei in the surroundings. So, IONPs as a CA affect the signal output of the magnetic nuclei

How to cite this article: Homeira F. Physicochemical Transformation Effect on the Relaxivity Enhancement of Iron Oxide Nanoparticles in Biomedical Imaging. Biostat Biom Open Access J. 2023; 11(2): 555810. DOI: 10.19080/BBOAJ.2023.11.555810

nearby. The magnetic properties of IONPs play a crucial role in the mechanism of relaxation enhancement. This mechanism is related to the magnetic centers and water molecules since the interaction of the water molecules and magnetic features of IONPs can affect the magnet center of it, thus enhancing the relaxation time. The distinctive features of IONPs, such as their uniformity and unique structures, are very important since one of the characterizations of it such as size can influence the IONPs [11]. Many review papers reported on the advantages of using IONPs for MRI purposes, but there are few review articles discussing the structure-relaxivity relationships of IONPs and their implications in MRI response. Theories such as Solomon-Bloembergen-Morgan (SBM) and the outer-sphere quantum mechanical help us to design the CA since the main purpose of these theories is related to the proton-electron interaction occurring between water protons. In the following section, we will discuss these two theories in detail.

SBM theory describes the T_1 relaxation enhancement based on the magnetic properties of the paramagnetic molecules. IONPs have a strong magnetization in the outer-sphere contributing to T_1 relaxivity. These nanoparticles are inversely related to size, meaning a smaller size leads to a higher magnetic surface since using water proton coordination and chemical exchange can provide a higher number of surface magnets. On the other hand, T_2 dephasing affecting leads to T_1 recovery of magnetization during the transition of the longitudinal times to the transverse direction [26]. It means T_1 recovery is susceptible to the T_2 dephasing effect. If we have transverse field fluctuation near the Larmor frequency, we will have T_1 relaxation enhancement. This is the main reason that IONPs show T_1 contrast at high magnetic fields. IONPs with the size of 3 nm in diameter have an efficient T_1 contrast agent ability. We can determine T_1 relaxivity not only by the size-dependent surface-to-volume ratio of IONPs but also by reducing the size of magnetic nanoparticles (MNPs) [27]. This is because by reducing the size of these, the surface energy of IONPs will increase and the colloidal stability in the environment will be decreased [25,28]. Based on an analysis of T_1 relaxivity by Shen et al, among different nanoparticles, the T_1 relaxivity of those that have a size below 5nm exhibited the highest r_1 times [28]. In general, the size of 3.6nm of IONPs has the lowest r2/r1 ratio and high T_1 contrast in imaging [28]. One of the significant bases of signal processing in MRI is that by shortening the T_2, the T_1 signal will happen. This cannot be obtained by decreasing the size of IONPs and altering the T_2 relaxivity since the r_1 value is still smaller than the r_2 value in this situation, even if the IONPs are too small. So, to obtain a T_1 signal, the T_2 should be diminished [29]. In general, the size depends on the optical and structural properties of IONPs, which are related to the electrical structure and quantum size of the nanoparticles. The synthesis method can affect the size and structure of the crystal. Consequently, the structural features of IONPs are too significant since the MRI contrast enhancement effect of IONPs is attributed in large part to their structural features [30].

Outer-Sphere Diffusion Model

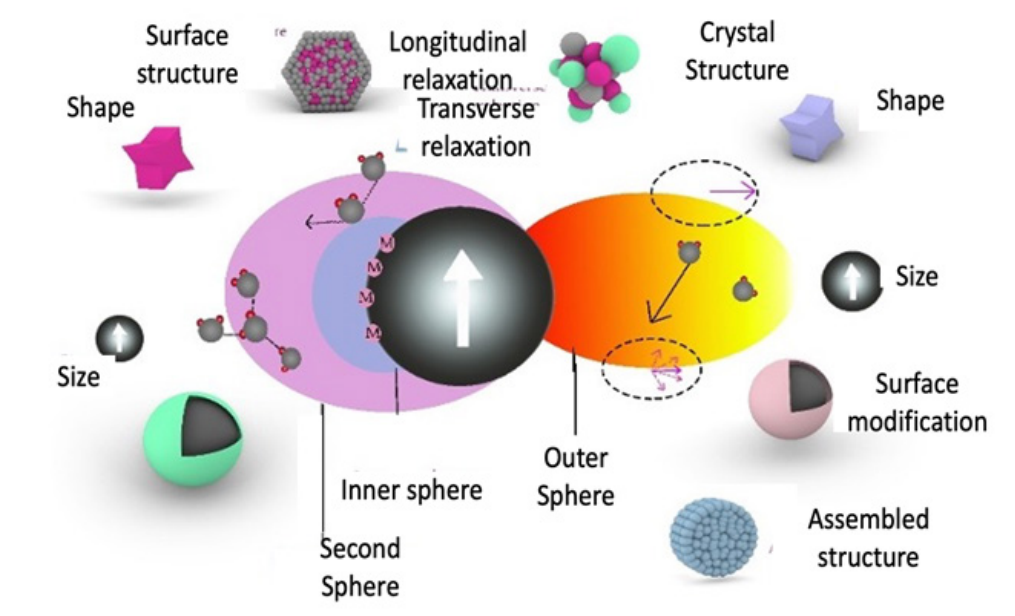

Figure 2: Schematic diagram of MNPs in interaction with water molecules. This schematic shows the structures of the inner spheres and the second sphere, which are predominantly long-relaxed (T1) of water molecules, which show the direct chemical exchange and hydrogen bonding models of MNPs' water molecules, respectively. MNPs are mainly characterized by structural features including size, shape, assembled structure, crystal structure, and surface properties that are summed up by increasing the relaxation on water protons. [Reproduced with permission from [35]. Copyright 2019, Advanced Materials].

How to cite this article: Homeira F. Physicochemical Transformation Effect on the Relaxivity Enhancement of Iron Oxide Nanoparticles in Biomedical Imaging. Biostat Biom Open Access J. 2023; 11(2): 555810. DOI: 10.19080/BBOAJ.2023.11.555810

In fact, the relaxation phenomenon in the outer-sphere theory is weak for magnetic particles. In this model, the dispersion of water molecules does not increase the relaxation time [31]. In fact, the dispersion of water without coordination with the magnetic centers is the main source of water movements [32]. Advances in nanotechnology, especially in superparamagnetic nanoparticles (SPNPs), together with single or multiple structures, create new phenomena in increasing relaxation in MRI. Nanoparticles such as SPNPs are able to generate a magnetic field under a large and susceptible external magnetic field at room temperature [33]. As a result, this magnetic field disrupts the phase coherence of water protons by reducing the relaxation time of T_2. (Figures 2A & B) you often do not use parentheses for figures. Please double-check the inconsistency. This T_2 relaxation, which is the interaction that occurs when water is dispersed, is called spin-spin relaxation. The quantum-mechanical theory is also valid for SPNPs as long as the particles are small enough to provide the conditions for the motional averaging regime (MAR) [34] (Figure 2).

The outer sphere model does not sufficiently define the relaxation profile. The best definition of relaxivity time is when it has both second sphere and outer-sphere models. Because the contribution of the second-sphere mechanism to relaxation is negligible, it is limited to certain cases where the inner-sphere has no coordination with water molecules. Consequently, 10-30% of the second-sphere mechanism can help relaxivity r_1. Molecules are generally subjected to three movements: vibration, transfer, and rotation. Transition motion is averaged in a homogeneous field, vibrational motion affects relaxation because of its velocity, and only rotational motion occurs at a range of frequencies that covers the Larmore frequency of protons in nuclear magnetic relaxation. These conditions can be met in many biological systems. For example, T_1 relaxation time is shorter than that of free water molecules in aqueous molecules that bind to proteins or macromolecules. The relaxation time of T_2 relaxation decreases the motion of water molecules as well as the average effect. A key feature that explains why paramagnetic materials are so effective at increasing proton relaxation is that gamma electron spins are more than 360,000 times the difference between electro-proton and proton-proton interactions because γ electron spins are more than 600 times larger than proton spins.

CA T_1 Proton-electron interactions between water protons and paramagnetic ions/molecules are the central mechanism of paramagnetic materials. In the classical model, water protons interact with paramagnetic centers and are classified into inner, second, and extraterrestrial mechanisms (Figure 4). The mechanism of the inner sphere is shown as chemical exchange, which involves the interaction of bulk water protons and the direct coordination of water protons with paramagnetic ions (Figure 4). The mechanism of the inner sphere is also shown as chemical exchange, which involves the direct coordination of water protons with paramagnetic ions after separation by interaction with bulk water protons. Based on the definition of chemical exchange, the transfer of a nucleus can occur either intra-molecularly or inter-molecularly, describing from one part of a molecule to another. In fact, it is the chemical exchange that shortens the relaxation times of T_1 and T_2 depending on the field. The mechanism of the inner sphere is modeled as follows, which dominates the increase of T_1 relaxation in paramagnetic CA.

$$T_{1e} = 1/25\Delta^2\tau_v[4S(S+1)-3][1/(1+\omega_s{}^2\tau^2{}_v)+4/(1+\omega_s{}^2\tau^2{}_v)] \quad (1)$$

$$T_{1e} = 1/25\Delta^2\tau_v[4S(S+1)-3][5/(1+\omega_s{}^2\tau^2{}_v)+2/(1+4\omega_s{}^2\tau^2{}_v)+3] \quad (2)$$

Where S is the total electron spins of the metal ion, ω_S is the angular electronic frequency, and T_{ie} is the electronic relaxation times (i = 1, 2); Δ is the zero-field splitting (ZFS) energy, and τ_v is the splitting correlation time.

Physicochemical factors affecting the relaxivity response in iron oxide nanoparticles

There are some contributing factors that affect r_1 and r_2. By using Equation 1, the relaxation value of r_i can be calculated [36]. For T_2 CA, contrast often results from fluctuations in the heterogeneity of magnetic slopes, making r_i^{SS} the most important contributor. On the other hand, for T_1 CA, more relaxation depends on the dipole-dipole coupling between the paramagnetic ions and the hydrogen nuclei, and the main influence is usually r_i^{IS} [37].

$$r_i = r_i^{IS} + r_i^{SS} + r_i^{OS} \quad (i=1,2) \qquad (3)$$

Equation 3 can have expended to access T_1 relaxation (Equation 4-6), where q^{ss} is the hydration number of the secondary intermediate sphere, q is the inner sphere hydration number, and T_{1m} and T_{1m}' are the T_1 relaxation times of water protons in the inner and second spheres, respectively; μ_0 is the Bohr magneton constant, τ_m and $\tau_{m'}$ are the residency times of water molecules in the inner and second spheres, g_e is the electronic g-factor, S is the spin quantum number of the corresponding paramagnetic species, γ_H is the gyromagnetic ratio of the proton, τ_c is the correlation time, τ_R is the rotational correlation time of the CA, and T_{1e} characterizes the electronic T_1 relaxation process [36,38].

$$r_1 = (Q/[H_{2O}])/T_{1m}\tau_m + (q^{SS}/[H_{2O}])/(T'_{1m}+\tau'_m) + r_1^{os} \quad (4)$$

$$1/T_{1m} = (2/15)(\mu_0/4\pi)(\gamma H^2 ge^2\mu B^2 S(S+1)/(r^6{}_{CH})[3\tau_c/1\omega^2{}_H\tau^2{}_c] \quad (5)$$

$$1/\tau_c = 1/\tau_m + 1/\tau_R + 1/\tau_{1e} \qquad (6)$$

Theoretically, the contrast factor T_1 is caused by a radio frequency disturbance produced by a variable magnetic field due to the fall of a paramagnetic component. Species with a large number of unpaired electrons are preferred because they have a large number of S contrast factor T_1. Most metal ions (Fe^{3+}, Mn^{2+}, Gd^{3+}) that have rich compounds of unpaired electrons have a greater ability to generate a strong magnetic field oscillation field [36,38].

How to cite this article: Homeira F. Physicochemical Transformation Effect on the Relaxivity Enhancement of Iron Oxide Nanoparticles in Biomedical Imaging. Biostat Biom Open Access J. 2023; 11(2): 555810. DOI: 10.19080/BBOAJ.2023.11.555810

Because the distance between water molecules and the center of contrast as well as their lifespan is high, the contribution of r1ss based on T_1 is usually negligible. Increased relaxation is possible by decreasing the pH and temperature, which in turn increases the q^{SS} and prolongs the residence of water protons in the secondary sphere [38]. For metal chelates, increasing r_1^{ss} can help improve hydration in the middle sphere by including polar donor groups such as phosphonates.

Hydrophobic monohydrate often increases the r_1^{ss} value when bound to the protein surface due to the presence of longer-lived water protons in the secondary sphere. Similarly, in Magnetic Hydration [39], in addition to the factors mentioned, a high surface-to-volume ratio that increases water access is also desired. For this reason, very small nanoparticles, as well as nanoparticles with reduced surface anisotropy and shape, are more desirable field [36,40]. As shown in equations 6-8, controlling parameters such as water dynamics time in the rotational motion of the CA, different surfaces, and different specific relaxation times, including (τ_m, τ_m, τ_R, and T_{1e}) increases the contrast performance [41].

All of these variables depend on factors including chemical and physical properties in the reaction between the CA, the aqueous environment, the molecular structure of the CA, and the magnitude of the external magnetic field. All of these affect the relaxation of the CA in a complex way [42]. When exposed to external fields of 1.5 T or higher, the electron relaxation is slowed because T_{1e} increases with the square of the field strength, and the relaxation depends more on the rotational motions ($1/\tau_R$) or the water exchange rate [38]. Theoretically, a convincing relaxation time is in equation 6. In a conventional MRI scanner with a magnetic field of 1.5 T or higher, τ_R is much smaller than τm and T_{1e}. Therefore, $\tau_R \approx 1/\omega_H$ is a necessary but insufficient factor. In fields less than 1.5 T, a slower motion is observed compared to those in higher fields of 7 T. There are two important strategies when nanoparticle macromolecules create. The first is to change the size of the nanoparticles or the weight of the molecules or macromolecules that are highly proportional to the magnetic field. The second is to adjust the stiffness of the structure [43].

The rate of water change ($1/\tau_m$ and $1/\tau_m$) also affects r_1. The range of τ_m is from 0.1 ns to tens of microseconds depending on the local coordination environment. To calm the inner sphere, τ_m r_1 is much shorter than T_{1m}, which means that water molecules are released before complete relaxation. For nanoparticles, it is possible to adjust the chemical environment to increase r_1 [42].

T_2 relaxation occurs through three mechanisms: dipole-dipole coupling between water hydrogen nuclei and metal ions, contact relaxation, and Curie spin relaxation. Based on equation 7, the Curie spin relaxation (r_2C) is created from dipolar interaction between static, magnetic, and dipolar interaction, where B is the magnetic field, C_0 is the Curie constant, and the function of the water diffusion correlation time (τ_D) [36,41]. In larger-sized CA (3-7 nm or larger), the $\varphi(\tau_D)$ decreases and the Curie spin becomes small [36,41]. The Curie spin relaxation is dominant between high field strength and small particle-sized contrast agents due to high magnetized CA and short τ_D [41].

$$r_2^C = C_0 B^2 \varphi(\tau_D) \quad (7)$$

Nanoparticles of high-saturation magnetic (SM) materials are made and can affect large volumes of water and are also able to effectively induce field heterogeneity. Despite the amount of magnetism, the more effective nanoparticles are often smaller than the material [36] (Figure 2C). One of the main reasons is the increase in magnetic anisotropy. An important factor of r_2 is the inhomogeneity caused by the CA, which is highly dependent on the magnetism of the CA [42]. In the spherical NPs mentioned, it is commonly seen in spherical particles that the surface-to-volume ratio is high because of the impact of surface magnetic anisotropy with smaller particles compared to much larger particles. Due to the presence of a 1 nm tilted layer at the particle surface, the spin state is greatly weakened because the magnetic moment is decreased, and the magnetic anisotropy is increased [36]. In addition to the effect of size, magnetic anisotropy also affects the shape of the structure, fine architecture, and surface coverage of nanostructures. For particles of the same volume, the anisotropy of the shape decreases with volume, increasing its magnetism and improving the similarity of the spin state between the surface and the core.

When two or more magnetic phases are in contact with each other, the bonding of displacements through collisions causes more anisotropy but increases their magnetic stability, which is often seen in nucleus shell nanostructures. Conversely, based on equation 6, nanoparticles that are non-spherical such as octopus' cubes and rods have more M_S than their spherical counterparts [44]. The use of coatings to protect nanoparticles from surface oxidation is very important because when the surface of nanoparticles disappears, their magnetic effect also disappears. Another very important factor for r_2 is the dynamic scattering of water molecules in the magnetic field gradient. This factor is measured by the number of water molecules scattered in the secondary sphere of the CA during their stay in the region. Therefore, the heavy water molecules contribute and oscillate. Therefore, a long time in the space adjacent to the magnetic field [39] (need a verb). Hence, nanoparticles with a larger magnetic field are more useful because they have a greater penetration region [45].

$$1/T_2 = (256\pi^2/405).\gamma^2 V^* M^2{}_s.d^2]/D(1+L/d) \quad (8)$$

Surface coating is also an important factor for T_2 in addition to the intrinsic property, size, and magnetic properties of nanoparticles. If the surface coating is inadequate, it may impede

How to cite this article: Homeira F. Physicochemical Transformation Effect on the Relaxivity Enhancement of Iron Oxide Nanoparticles in Biomedical Imaging. Biostat Biom Open Access J. 2023; 11(2): 555810. DOI: 10.19080/BBOAJ.2023.11.555810

water diffusion or prolong the residence of water, remove water from the nanoparticle surface, and ultimately reduce the contrast. They protect against unwanted destruction or accumulation and have good colloidal stability. A hydrophilic surface is preferred for nanoparticles because it shows the importance of changes in the surface of nanoparticles after synthesis and supports the diffusion of water molecules in the second sphere [46]. In fact, bond density, coating porosity, fine-tuning of coating thickness, and transfer of a layer of hydrolytic coating to the particle surface [45].

There are several types of IONPs, the most important of which are Fe_3O_4 and Fe_2O_3. Manipulation of reaction parameters is essential to achieving controlled nanoparticles. These manipulations include shape, size, morphology, crystallization, and purity. All of these paths are very difficult. In the production of IONP based on T_1 CA, the core and surface of IONP coatings play a very important role in contrast. Size and shape must be controlled because they determine the phase, crystallization, size, and magnetism of the IONP. Size refers to both the hydrodynamic size (core+ coating) and the size of the core. In general, a smaller core is better for positive T_1, and when the size is less than 5 nm, single magnetic amplitudes are reduced. This causes it to create the effect of spin and the formation of unpaired electrons of Fe^{3+} and Fe^{2+} which will have more paramagnetic particles than superparamagnetic ones (Figure 2). As the nanoparticle size decreases, it is directed towards paramagnetic or superparamagnetic magnetization because decreasing the size leads to increases in the superparamagnetic behavior and decreases the ferromagnetic behavior. Therefore, the focus on oxygen decreases and there is a slight decrease in iron balance [47] (Figure 3).

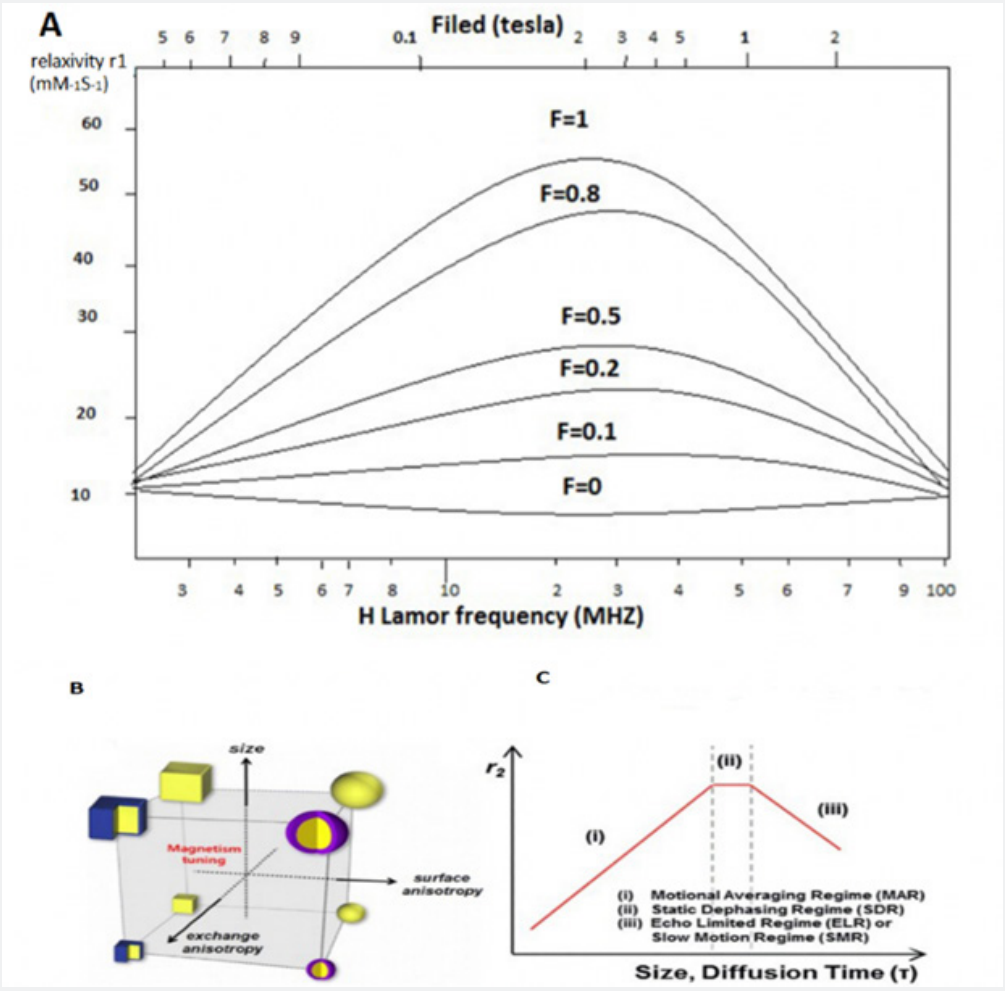

Figure 3: (a) Simulation of r1 over a range of Larmor frequencies (ωH) for contrast complexes using a Lipari-Szabo model-free approach. The resulting r1 increases as the structural flexibility (described by factor F) decreases (i.e., F = 0 corresponds to flexible, free molecules, and F =1 corresponds to a rigid structure with no flexibility). (b) An NP that can reduce magnetic anisotropy by increasing particle size and reducing surface/shape anisotropy with a large magnetization. (c) Three distinctive regimes, such as: (i) MAR, (ii) SDR and (iii) SMR of outer sphere relaxation theory. [Reproduced with permission from [36]. Copyright 2018, Royal Society of Chemistry].

How to cite this article: Homeira F. Physicochemical Transformation Effect on the Relaxivity Enhancement of Iron Oxide Nanoparticles in Biomedical Imaging. Biostat Biom Open Access J. 2023; 11(2): 555810. DOI: 10.19080/BBOAJ.2023.11.555810

There are different relaxation properties for MRI: T_1 (spin-lattice or longitudinal relaxation), T_2 (spin-spin or transversal relaxation), and T_2^*. T_2 relaxation time creates a signal-to-noise ratio and causes contrast between soft tissues. In MRI, the main effect of SPIO particles is on the relaxation of T_2^*, which is caused by the use of T_2/T_2^* weight sequences. This also creates the loss of tissue signal due to the effects of iron oxide nucleus sensitivity. Additionally, soft tissues have various cellular composition and density, which corresponds to different T_1 and T_2 relaxation times. (Table 1) shows the different values of relaxation time in different tissues in the magnetic field [48] (Figure 4).

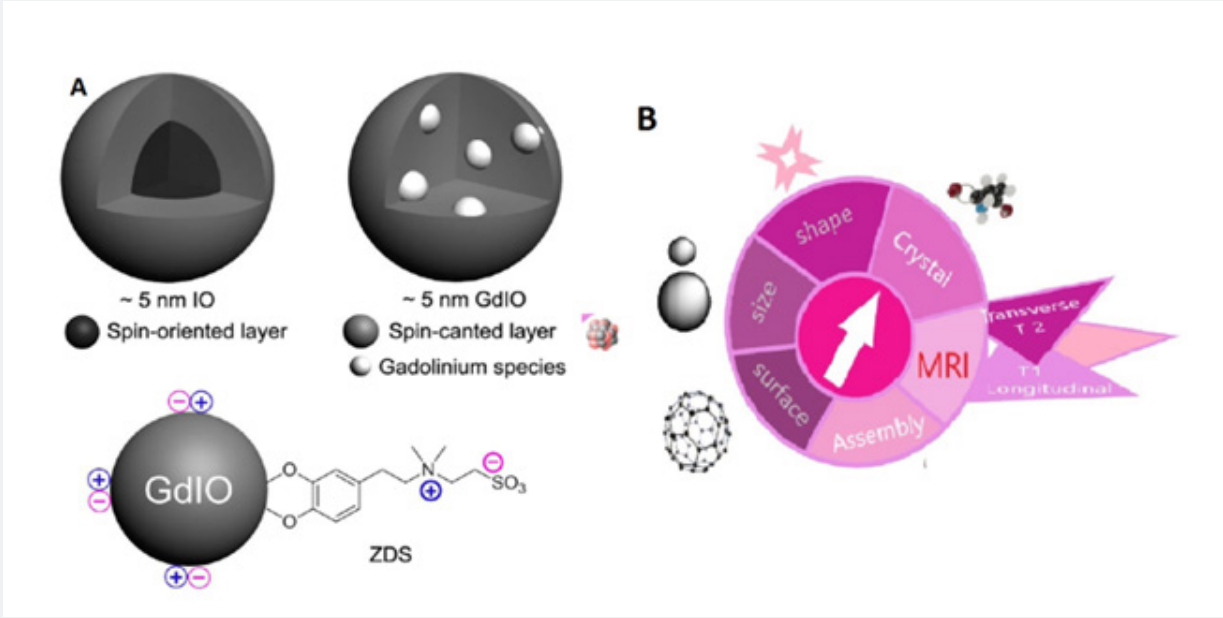

Figure 4: (a). T1, T2 relaxation time directly affects the feature of the nanoparticles. Effects of the different features of using CA such as size, shape, crystal, surface, assembly, and coating on MRI. (b). Small sized (below 5 nm in diameter) GdIO NPs with inner spin-canting effect.

Table 1: Typical relaxation times values of some human tissues at clinical magnetic fields.

		1.5T				3T			
Tissue min		T_1(ms)		T_2(ms)		T_1(ms)		T_2(ms)	
		max	min	max	min	max	min	max	
Brain	Grey matter	1260.8		109.4		1600		92.6	
		1096.5	1531	77.9	217	1275	1763	66	110
		1124±50		95±8		1820±114		99±7	
		1150		100		1600		70	
		960				1331			
	White matter	999.9		112.3		1100		60.8	
		612	1587	66.2	282	812.3	1110	49.5	79.6
		800		80		1100		60	
		700				832			
		884 ±50		72 ±4		1084±45		69 ±3	
Skeletal muscle		1008±20		44±6		1412±13		50± 4	
	1000		35		1400		30		
	981.5		36		1232.9		37.2		
	860-1130				900-1420				

How to cite this article: Homeira F. Physicochemical Transformation Effect on the Relaxivity Enhancement of Iron Oxide Nanoparticles in Biomedical Imaging. Biostat Biom Open Access J. 2023; 11(2): 555810. DOI: 10.19080/BBOAJ.2023.11.555810

Size

The size factor was first considered before the theory of quantum confinement. The relationship between nanoparticles' size and magnetic properties has been widely reported [49]. The role of nanoparticles is considered both positive and negative in MRI [50]. In the SBM theory utilized in paramagnetic metal-chelating systems, the gap between paramagnetic systems and nanoparticles in terms of size effect must be considered. Size is an important factor that affects the T_1 and T_2 relaxivity of nanoparticles separately. It is significant to mention that the level of interdependence with T_1 and T_2 relaxivities can be observed (i.e., factors affecting T_1 also affect T_2 relaxivity in MRI) [51]. The magnetism of an NP is the sum of all the magnetic moments within the sample, divided by the volume of the sample. This value is independent of the grain size [52]. In general, larger nanoparticles have a higher r_2 value in MAR [25]. The value of r_2 is positively correlated with the diameter of the IONP. T_2 relaxivity is dependent on the size for different types of nanoparticles including their alloy. When MNPs reach the critical size limit of MAR, the size-dependency of T_2 relaxivity ends. Because the emission of protons around nanoparticles is still related to the discharge of the magnetic core, it is no longer as dependent on the size of the nanoparticles (Figure 4) [53]. It then becomes dependent on the static dephasing regime (SDR) or slow-motion regime because the diffusion of protons around the nanoparticles will not be able to perform the various phases of the nucleus under the static field inhomogeneity on average. T_2 relaxation decreases with decreasing nanoparticle size; as the NP size decreases, the T_2 relaxation also decreases. This is attributed to the emission of finite protons at a time interval between a pulse-echo pair [25]. As a result, SDR theory plays an important role in the formation of MRI signals by echo gradient sequence [39].

It has been shown that the effect of T_1 relaxation amplification is based on the paramagnetic model. Unlike paramagnetic macromolecules, nanoparticles are considered strong magnetic systems (Figure 4). Smaller nanoparticles provide more magnetic metals to coordinate water protons and chemical exchange. The surface ions of nanoparticles can be described in terms of surface-to-volume ratio because they are inversely related to size [31] . However, due to the transmission of the longitudinal signal to the transverse direction during the measurement of T_1, it is very sensitive in the recovery of the T_1 relaxation time [36]. Paramagnetic IONPs can be obtained without size effect using the ultra-low field (ULF) or higher magnetic field [52]. Interestingly, it has been shown that SPIONs could be used to increase the contrast strength of T_1 in ULF-MRI by adjusting the oscillations of magnetic nanoparticles. The effect of adverse negative contrast greatly reduces the unsaturated magnetic moment of SPIONs in ULF [54] (Figure 5).

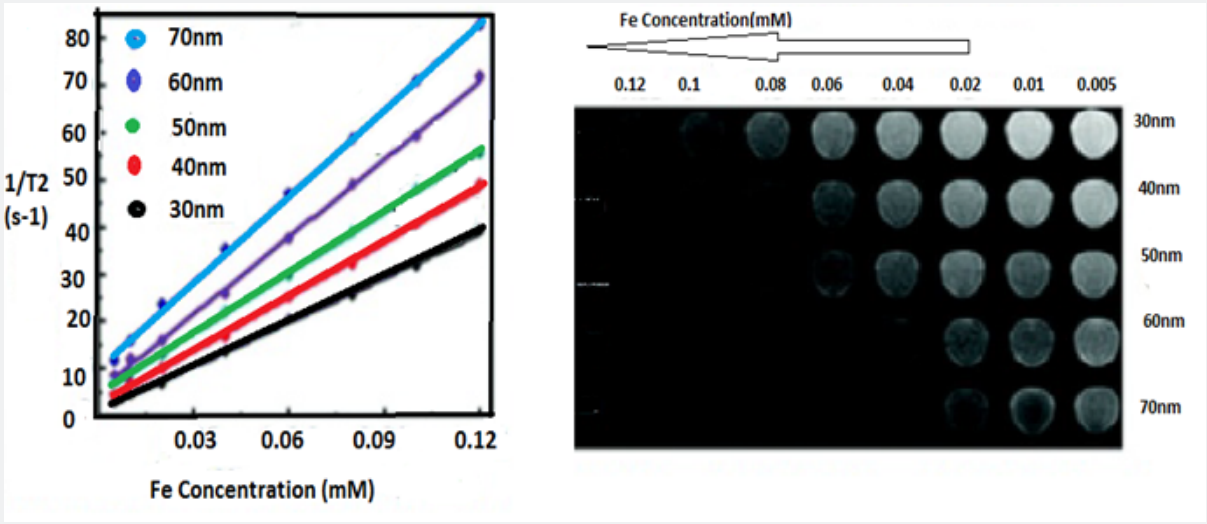

Figure 5: The MR contrast effect of Fe3O4 NRs of different lengths and NPs of different diameters. [Reproduced with permission from [76]. Copyright 2018, Theranostic].

Shape

Nanoparticles are composed of magnetic moments of separate but strongly interacting bundles [55]. The control and design of nanoparticles is not only an aesthetic mode, but also a starting point for applications such as functional design, sensors, and analysis. There are many classical theories about the shape of nanoparticles, including the classical theory of electrodynamics, which shows that the elliptical shape has a homogenous magnetic field, but the distortion of the shape requires additional energy to stabilize the anisotropy of the particles. The shape of nanoparticles is another important factor that determines the strength and specificity of magnetic anisotropy. There is a need for more precise control of synthetic methods in strong oxygen-metal bonding and various crystal packing structures in IONPs crystals (Figure 6).

How to cite this article: Homeira F. Physicochemical Transformation Effect on the Relaxivity Enhancement of Iron Oxide Nanoparticles in Biomedical Imaging. Biostat Biom Open Access J. 2023; 11(2): 555810. DOI: 10.19080/BBOAJ.2023.11.555810

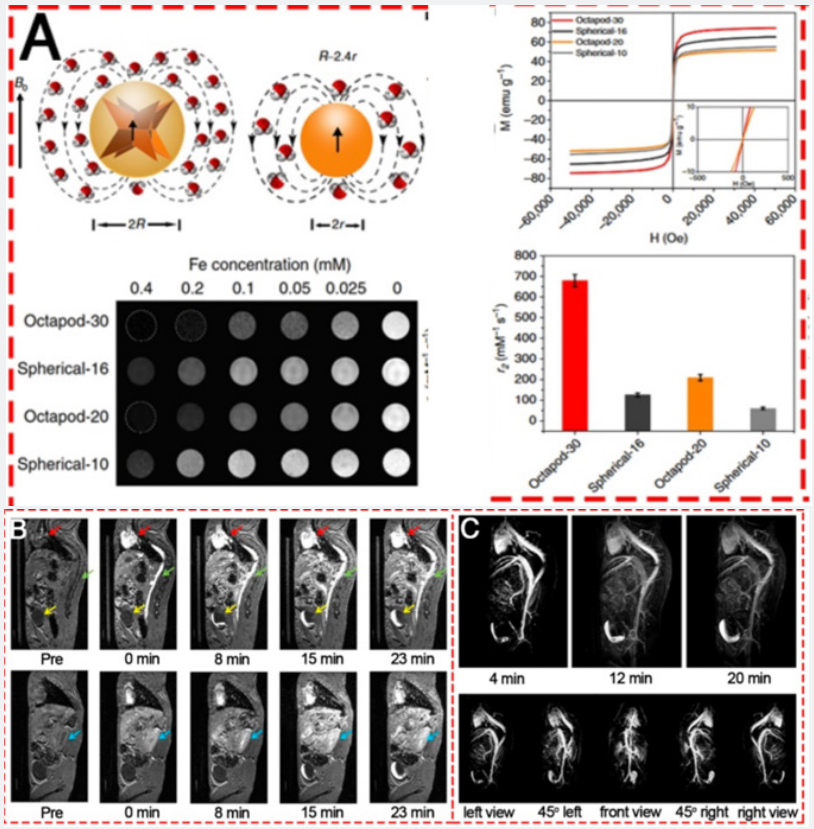

Figure 6: (a). T2-weighted contrast MR images of various IONPs. (A) Schematic illustration of the ball models of octapod and spherical IONPs with the same geometric volume, smooth M–H curves, T2-weighted MR images, and comparison of r2 values of IONPs with different diameters: Octapod-30 (~58 nm), Octapod-20 (~49 nm), Spherical-16 (~30 nm) and Spherical-10 (22 nm). (b). T1-weighted MR images of a mouse injected with ZDS-coated exceedingly small SPIONs (ZES-SPIONs) at 7 T. (c) T1-weighted MRA of a mouse injected with ZES-SPIONs at 7 T. [Reproduced with permission from [52]. Copyright 2018, Theranostic].

Cubes

One novel idea that has been developed as an approach to synthesizing nanoparticles over the past few decades makes use of an elliptical deformation [24]. What has yet to be shown is to what extent this deformation affects the magnetic properties of nanoparticles. Different recent studies have used a variety of shapes of nanoparticles including cube, concave, octahedron, tripod, plate, flower, octagon, and quadrilateral [56]. In general, nanoparticles are denser in the vertical direction of the particle than in the spherical equivalent and produce a local magnetic field that extends farther in the direction parallel to the particle magnetization [34]. Due to the well-defined shape and structure, the T_1 relaxation capability and the T_1-T_2 contrast mode can be increased. The cube shape is an especially exceptional model that provides to investigate the effect of surface structure on the T_1 relaxation of nanoparticles.

Octopods

Gao and his colleagues have recently developed an octopod model, which suggests that the shape of the non-spherical nanoparticles may create a larger area of spin turbulence than spherical nanoparticles. Although the outer-sphere diffusion classical theory coefficient is included in the volume fraction, the radius applied to define the T_2 relaxivity of nanoparticles is simulated based on the spherical shape [51]. Additionally, researchers have recently shown that tripod IONPs increase T_2 relaxivity, and also shortly before that the effective radius was investigated [57] (please double-check this sentence). Decomposition of iron oleates in the presence of chloride (NaCl) results in the production of Octapod iron oxide nanoparticles. Briefly, at 320°C, iron oleate is decomposed in Octadeson solvent for 2 hours. Transmission TEM electron microscope images according to Figures 6a & b. show that the high-performance product (495%) is composed of iron oxide particles such as uniformly four-armed stars. The average edge length between two armed points is about 30 nanometers. (Figure 6c) shows the uniform lattice margins of the whole nanoparticles with a high-resolution Fe_3O_4 (220) distance. Upon closer inspection of

How to cite this article: Homeira F. Physicochemical Transformation Effect on the Relaxivity Enhancement of Iron Oxide Nanoparticles in Biomedical Imaging. Biostat Biom Open Access J. 2023; 11(2): 555810. DOI: 10.19080/BBOAJ.2023.11.555810

these nanoparticles, shadows belong to the four arms of star-like particles, indicating the presence of a concave property in the particles (Figure 7).

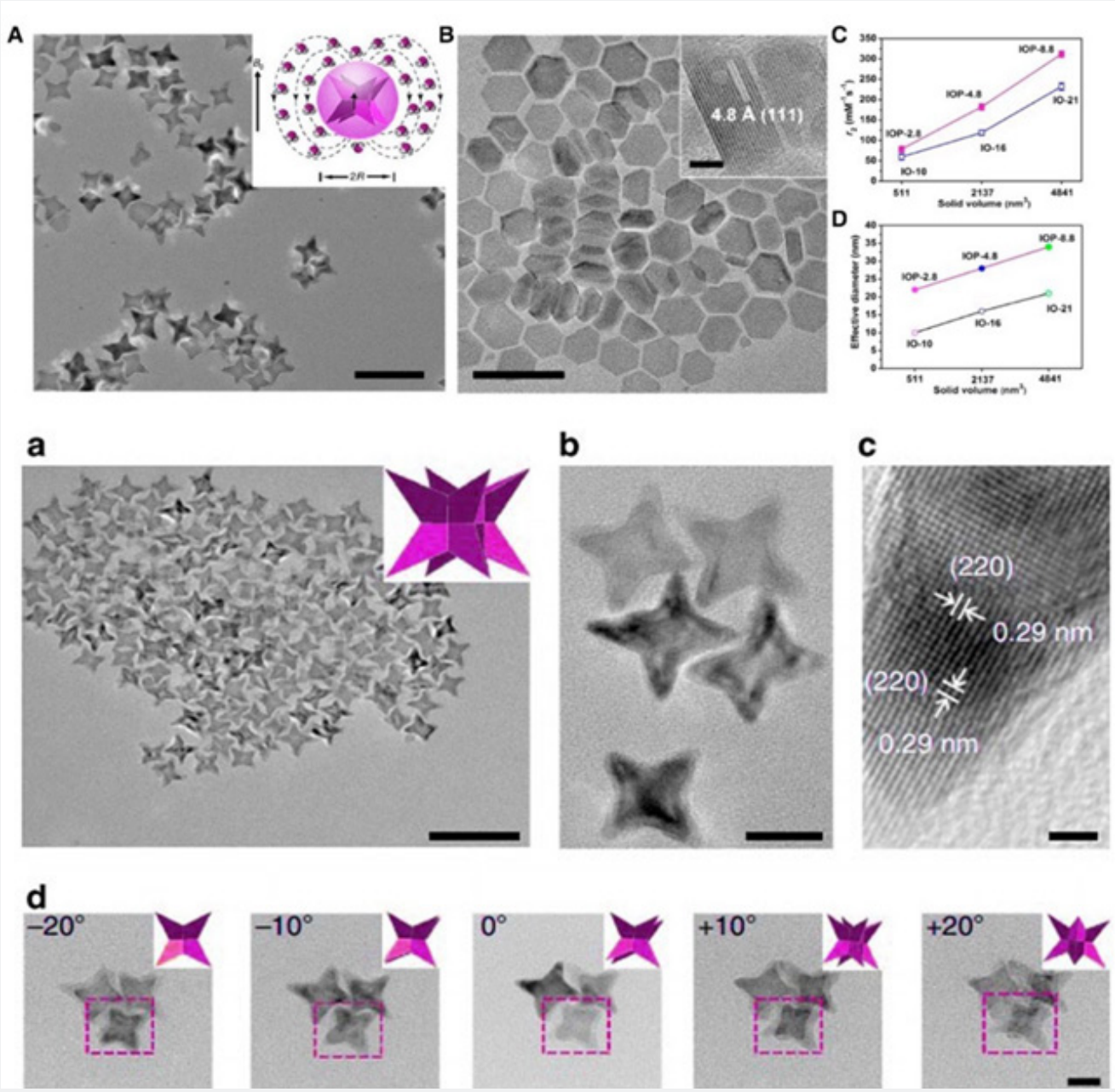

Figure 7: Top. (a) Due to reduced surface/shape anisotropy, octapod IONPs are capable of generating a larger volume of magnetic inhomogeneity than spherical particles with the same geometric volume. Scale bar, 100 nm. Adapted with permission from [57], copyright 2013 Springer Nature. (b) TEM images of 2D-Fe3O4 nanosheet with a thickness of 8.8 nm. Scale bar, 100 nm (insert, 5 nm). 2D-Fe3O4 nanosheets exhibited higher r2 values (c) and larger effective diameters (d) than IONPs of equivalent surface area. Scheme of TEM analysis of Octapod-30 iron oxide nanoparticles. Bottom. (a) The TEM image of the Octapod-30 is composed of uniform, four-armed star particles. (b) Magnification of the TEM image of the Octapod-30 (c). The TEM image of Octapod-30 is made up of whole nanoparticles that indicate single crystallization with lattice margins corresponding to Fe3O4 (202). (d). Diagonal images of Octapod-30. [Reproduced with permission from [58]. Copyright 2013, Natural communications].

How to cite this article: Homeira F. Physicochemical Transformation Effect on the Relaxivity Enhancement of Iron Oxide Nanoparticles in Biomedical Imaging. Biostat Biom Open Access J. 2023; 11(2): 555810. DOI: 10.19080/BBOAJ.2023.11.555810

Plates

Platelet structures of nanoparticles provide the conditions for the adjustment of tailor spin exchange interactions in magnetic devices. The magnetic exchange interactions in the thin layer structure create magnetic crystals. Therefore, the platelet structures of nanoparticles have attracted a lot of attention [31]. In Mn^{4+} ions, the value of r_1 is less than that of manganese oxide Nano plates with a passive surface of Mn^{3+} [58]. Recently, the Pearson instant correlation method has been used to show the high amount of r_1 paramagnetic manganese oxide Nano plates at the surface [55]. Optimal coordination and chemical exchange of water protons by deformation from sphere to plate affects the density of metal ions exposed to the surface (Figure 8).

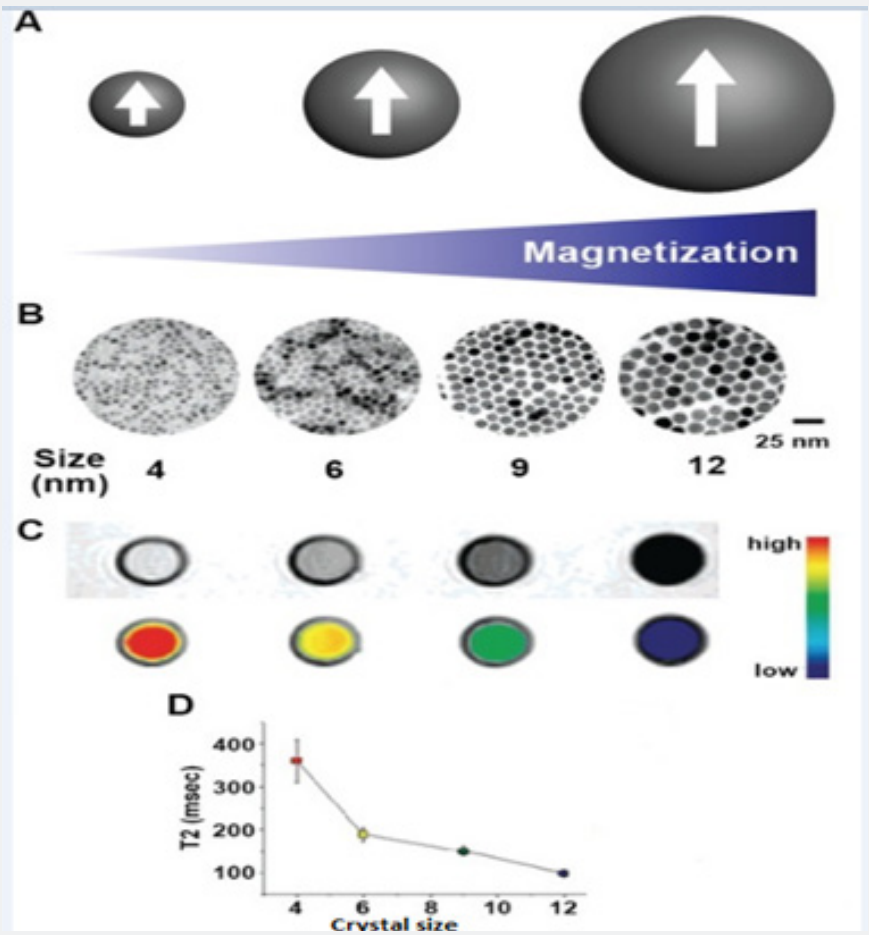

Figure 8: Size effect on T2 relaxivity of MNPs. (a) Cartoon showing size-dependent magnetization effect of MNPs. (b-c-d) TEM images, MR phantoms, relaxation times, and magnetizations of Fe3O4 nanocrystals with different diameters of 4, 6, 9, and 12 nm, respectively. [Reproduced with permission from [43]. Copyright 2019, Advanced Materials].

In general, in nanoparticles, there are crystals in the range of 20-150 nm referred to as SPIONs, including Fe_3O and maghemite γ-Fe_2O_3, , which exhibit an ultra-magnetic order. One of their characteristics is colloidal stability, which increases their activity level in aqueous media. These changes occur by coating SPION with organic acids or with a hydrophilic and biocompatible polymer [36]. They are capable of binding to a variety of biomolecules and can be used in a wide range of applications in tissue engineering and nanotechnology [59]. The average length of cubic SPIONs is 12 nm, which is the best recommended size for tissue diffusion. Cubic SPIONs are synthesized by thermal decomposition and their surfaces are modified with oleic acid. The physicochemical properties, structure, and type of SPIONs are usually studied using XRD diffraction, X-ray photoelectron spectroscopy, and more. A set of techniques for describing acid-modified SPIONs can be referred to as dynamic light scattering and nanoparticles tracking analysis [38].

This stage relies on a special arrangement of magnetic atoms and the alignment of magnetic moments, including simple and complex processes that relate to the crystal structure of the material, comprising the super exchange effect, the amplitude boundary, and the crystal anisotropy of the crystal phase. In

How to cite this article: Homeira F. Physicochemical Transformation Effect on the Relaxivity Enhancement of Iron Oxide Nanoparticles in Biomedical Imaging. Biostat Biom Open Access J. 2023; 11(2): 555810. DOI: 10.19080/BBOAJ.2023.11.555810

the next section, we will explain the relationship between the different properties of crystals and their magnetic properties, and their effects on the T_1 and T_2 relaxivities [60].

Magnetic Resonance-Computer Tomography bimodal imaging

For example, nuclear medicine imaging techniques are highly sensitive but have a low resolution. On the other hand, CT can perform several pathologies at a high speed, but the amount of dose received by the patient is High field [61-63]. The disadvantage of MRI is low sensitivity but a high ability to distinguish soft tissues from each other. As a result, multimodal imaging methods such as MR-CT or PET-CT can be used to overcome these limitations. Multimodality imaging techniques can gather all the morphology and anatomical information. It is referred to as multimodal imaging, which has advantages such as synergistic over any modality alone. Molecular imaging including PET-CT and PET-MR plays a vital role in understanding the patient's pathobiological principles [50,64,65]. Chemistry and medical imaging probes are now suitable imaging techniques by focusing on nanoparticle (NP)-based PET/MRI multimodal tracers in oncological imaging. A PET- MRI scanner consists of three components, namely a carrier, a PET tracer that is a radioisotope emitted from the patient's body with high sensitivity, and an MRI that produces high contrast and resolution. In MRI, nanoparticles (IONPs) can be used as CA [66].

The nanoparticles used in MRI have different designs, including particle size, charge, core, and surface properties, which are the main features that help reduce the toxicity of nanoparticles [66-69]. For example, the hydrodynamic size of nanoparticles determines their fate in the body. Particles with a diameter of less than 5 nanometers are absorbed, while particles with a larger diameter absorb from another organ in the body [70,71]. Also, the shape of the particles affects the internalization of the cell. In general, the properties of ligands and nanoparticles are very important in multimodal imaging, since a significant number of targeting probes are needed to track a specific biological path [72,73].

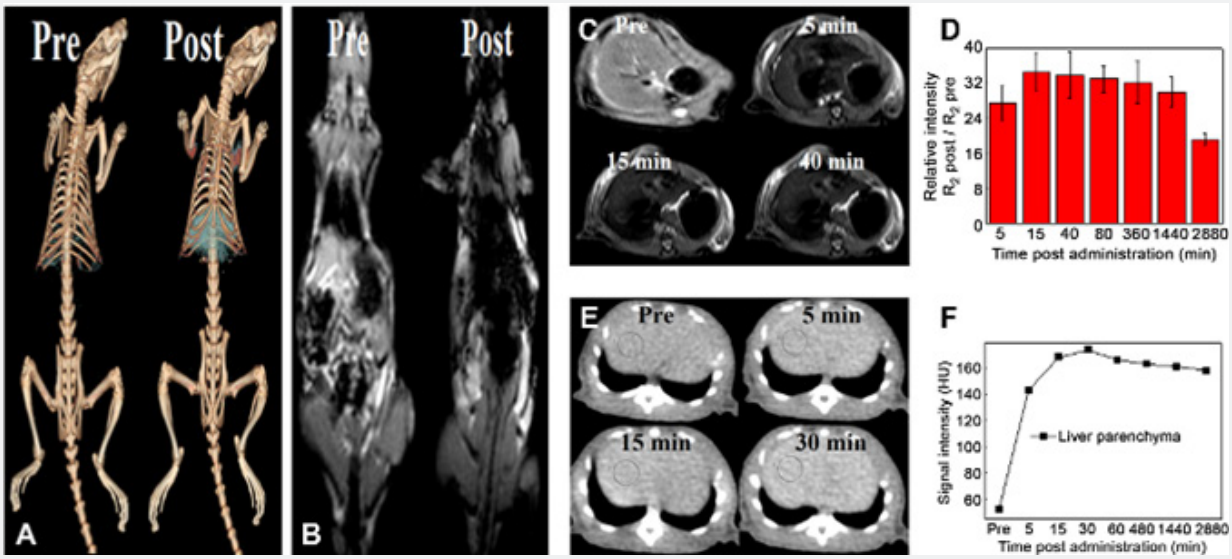

Figure 9: CT images of normal rat pre and post systematic administration of Fe3O4-Au NPs in (highlighted in E with black circles) in respect of HU values pre and post contrast. T2-weigh view. (D) Enhancement in liver parenchyma in respect of signal intensity. [Reproduced with permission from [76]. Copyright 2015, Scientific Reports.]

Additionally, properties like size, shape, crystal structure and surface coating will have a great impact on the relaxivity of the contrast agent. IONPs can also be used with other modalities like computed tomography (CT) and nuclear medicine imaging techniques like positron emission tomography (PET) and single-photon emission computerized tomography (SPECT)[1,80]. Because IONPs can be used in so many biomedical applications, it requires a well-thought-out approach when designing and researching a high relaxivity contrast agent (Figure 9).

Challenges in iron oxide-based CA

In SPION, size and morphology play a very important role in the depth of tissue penetration. The size of SPIONs will have the greatest penetration in the tissue when it is less than 10 nm. This size should be chosen to meet specific biomedical challenges [74]. The size should be small enough to pass by intravenous injection through the capillaries. It should be large enough to be manipulated by a magnetic actuator [43]. An example of this is

How to cite this article: Homeira F. Physicochemical Transformation Effect on the Relaxivity Enhancement of Iron Oxide Nanoparticles in Biomedical Imaging. Biostat Biom Open Access J. 2023; 11(2): 555810. DOI: 10.19080/BBOAJ.2023.11.555810

single spherical particles with a hydrodynamic diameter of 10-20 nm that are suitable for injection into samples but have limited magnetic mechanical effects, so SPIONs in the range of 100 nm can solve this problem [75].

Conclusion

The size and shape of the nanoparticles were controlled by PH, temperature, and concentration of reagents. But nanoparticles are generally poorly permeable, so their stability is a predicament [77]. Stability in biological environments remains a challenge30. In fact, although r_2 decreases with decreasing core size, the optimum size (r_2/r_1) reaches 3.6nm. Because IONPs suffer from smaller amounts of high-level energy, they accumulate and increase the value of r_2/r_1. As mentioned, deactivating smaller IONPs to stabilize biological environments is a challenge because smaller IONPs have lower saturation magnetization [78]. As a result, in order to minimize IONPs, r_2 must be smaller than the core size. The magnetic properties of magnetite and maghemite nanoparticles have been investigated by more than one research group. However, distinguishing magnetite from maghemite is a major challenge. X-ray diffraction (XRD) processing patterns are very similar [79].

References

1. Faridnejad H (2022) Evaluation of Radiation Risk and Protection of SPECT/CT Compared to SPECT Alone Journal of Microbiology and Biotechnology Reports 5(6): 64-66.
2. Naumenko V, Garanina A, Nikitin A, Vodopyanov S, Vorobyeva N et al. (2018) Biodistribution and Tumors MRI Contrast Enhancement of Magnetic Nanocubes, Nanoclusters, and Nanorods in Multiple Mice Models – PMC. Contrast Media Mol Imaging pp.1-12.
3. Emmanuel Garnier, Francisco JVI, Feliu JM, Gullon JS (2019) Surface Structure Characterization of Shape and Size Controlled Pd Nanoparticles by Cu UPD: A Quantitative Approach. Chemistry 7(1).
4. Faridnejad H (2022) The Impact of Physicochemical Modification on Iron Oxide Nanoparticle Relaxation Enhancement in Biomedical Imaging in The Anticancer Sector. Annals of Experimental Biology 10(2).
5. Lorenc T, Chrzanowski J, Olejarz W (2020) Current Perspectives on Clinical Use of Exosomes as a Personalized Contrast Media and Theranostics. Cancers 12(11): 3386.
6. Zhao Z, Li M, Zeng J, Huo L, Liu K (2022) Recent Advances in Engineering Iron Oxide Nanoparticles for Effective Magnetic Resonance Imaging. Bioactive Materials 12: 214–245.
7. Khan I, Saeed K, Khan I (2019) Nanoparticles: Properties, Applications and Toxicities. Arabian Journal of Chemistry 12(7): 908–931.
8. Ali A, Shah T, Ullah R, Zhou P, Guo M et al. (2021) Review on Recent Progress in Magnetic Nanoparticles: Synthesis, Characterization, and Diverse Applications. Frontiers in Chemistry 9(1).
9. Bantz C, Koshkina O, Lang T, Galla HJ, Kirkpatrick CJ et al. (2014) The Surface Properties of Nanoparticles Determine the Agglomeration State and the Size of the Particles under Physiological Conditions. Beilstein J Nanotechnol 5: 1774–1786.
10. Nguyen MD, Tran HV, Xu S, Lee TR (2021) Fe_3O_4 Nanoparticles: Structures, Synthesis, Magnetic Properties, Surface Functionalization, and Emerging Applications. Applied Sciences 11(23): 11301.
11. Kim BH, Hackett MJ, Park J, Hyeon T (2014) Synthesis, Characterization, and Application of Ultrasmall Nanoparticles. Chem. Mater 26(1): 59–71.
12. Bonvin D, Alexander DTL, Millan A, Pinol R, Sanz B et al. (2017) Tuning Properties of Iron Oxide Nanoparticles in Aqueous Synthesis without Ligands to Improve MRI Relaxivity and SAR. Nanomaterials (Basel) 7(8): 225.
13. Orlacchio A, Ciarrapico AM, Schillaci O, Chegai F, Tosti D et al. (2014) PET-CT in Oncological Patients: Analysis of Informal Care Costs in Cost-Benefit Assessment. Radiol Med 119(4): 283–289.
14. Gan YX, Jayatissa AH, Yu Z, Chen X, Li M (2020) Hydrothermal Synthesis of Nanomaterials. Journal of Nanomaterials pp.1-3.
15. Benhammada A, Trache D, Kesraoui M, Chelouche S (2020) Hydrothermal Synthesis of Hematite Nanoparticles Decorated on Carbon Mesospheres and Their Synergetic Action on the Thermal Decomposition of Nitrocellulose. Nanomaterials (Basel) 10(5): 968.
16. Maoquan Chu, Yuxiang Shao, Jinliang Peng, Xiangyun Dai, Haikuo Li, Qingsheng Wu (2013) Near-infrared laser light mediated cancer therapy by photothermal effect of Fe_3O_4 magnetic nanoparticles. Biomaterials 34(16): 4078-4088.
17. Cristina Blanco-Andujar, Aurelie Walter, Geoffrey Cotin, Catalina Bordeianu, Damien Mertz (2016) Design of iron oxide-based nanoparticles for MRI and magnetic hyperthermia. Nanomedicine 11(14).
18. Orlacchio A, Ciarrapico AM, Schillaci O, Chegai F, Tosti D et al. (2014) PET-CT in Oncological Patients: Analysis of Informal Care Costs in Cost-Benefit Assessment. Radiol Med 119(4): 283–289.
19. Schillaci O, Scimeca M, Toschi N, Bonfiglio R, Urbano N, Bonanno E et al. (2019) Combining Diagnostic Imaging and Pathology for Improving Diagnosis and Prognosis of Cancer. Contrast Media Mol Imaging pp. 9429761.
20. Hao Liu, Yao Chen, Shuang Wu, Fahuan Song, Hong Zhang et al. (2016) Molecular imaging using PET and SPECT for identification of breast cancer subtypes. Nuclear Medicine Communications 37(11): 1116-1124.
21. Johannes Grueneisen, James Nagarajah, Christian Buchbender, Oliver Hoffmann, Benedikt Michael Schaarschmidt (2015) Positron Emission Tomography/Magnetic Resonance Imaging for Local Tumor Staging in Patients With Primary Breast Cancer: A Comparison With Positron Emission Tomography/Computed Tomography and Magnetic Resonance Imaging: Investigative Radiology 50(8): 505-513.
22. Cristiano Rampinelli, Paolo De Marco, Daniela Origgi, Patrick Maisonneuve, Monica Casiraghi (2017) Exposure to low dose computed tomography for lung cancer screening and risk of cancer: secondary analysis of trial data and risk-benefit analysis. BMJ pp. 356.
23. Ding Song Yuan, Yi Jun, Li Jian Feng, Ren Bin, Wu De Yin et al. (2016) Nanostructure-based plasmon-enhanced Raman spectroscopy for surface analysis of materials. Nature Reviews Materials 1(6): 16021
24. Wu L, Mendoza Garcia A, Li Q, Sun S (2016) Organic Phase Syntheses of Magnetic Nanoparticles and Their Applications. Chem Rev 116(18): 10473–10512.
25. Zhou Z, Yang L, Gao J, Chen X (2019) Structure-Relaxivity Relationships of Magnetic Nanoparticles for Magnetic Resonance Imaging. Adv Mater 31(8): e1804567.

How to cite this article: Homeira F. Physicochemical Transformation Effect on the Relaxivity Enhancement of Iron Oxide Nanoparticles in Biomedical Imaging. Biostat Biom Open Access J. 2023; 11(2): 555810. DOI: 10.19080/BBOAJ.2023.11.555810

26. Zhou Z, Bai R, Munasinghe J, Shen Z, Nie L et al. (2017) T1-T2 Dual-Modal Magnetic Resonance Imaging: From Molecular Basis to Contrast Agents. ACS Nano 11(6): 5227–5232.

27. Dong H, Du SR, Zheng XY, Lyu GM, Sun LD et al. (2015) Lanthanide Nanoparticles: From Design toward Bioimaging and Therapy. Chem. Rev 115(19): 10725–10815.

28. Shen Z, Chen T, Ma X, Ren W, Zhou Z (2017) Multifunctional Theranostic Nanoparticles Based on Exceedingly Small Magnetic Iron Oxide Nanoparticles for T1-Weighted Magnetic Resonance Imaging and Chemotherapy. ACS Nano 11(11): 10992–11004.

29. Wang L, Lin H, Ma L, Jin J, Shen T et al. (2017) Albumin-Based Nanoparticles Loaded with Hydrophobic Gadolinium Chelates as T1–T2 Dual-Mode Contrast Agents for Accurate Liver Tumor Imaging. Nanoscale 9(13): 4516–4523.

30. Abe H, Naka T, Sato K, Suzuki Y, Nakano M (2019) Shape-Controlled Syntheses of Magnetite Microparticles and their Magnetorheology. IJMS 20(15): 3617.

31. Shuai M, Klittnick A, Shen Y, Smith GP, Tuchband MR et al. (2016) Spontaneous Liquid Crystal and Ferromagnetic Ordering of Colloidal Magnetic Nanoplates. Nat Commun 7: 10394.

32. Zhao F, Liu L, Yang Y, Zhang R, Ren G (2015) Effect of the Hydrogen Bond on Photochemical Synthesis of Silver Nanoparticles. J Phys Chem A 119(50): 12579–12585.

33. Lopez Neira JP, Galicia Hernandez JM, Reyes Coronado A, Perez E, Castillo Rivera F et al. (2015) Surface Enhanced Raman Scattering of Amino Acids Assisted by Gold Nanoparticles and Gd(3+) Ions. J Phys Chem A 119(18): 4127–4135.

34. Sinmyo R, Bykova E, Ovsyannikov SV, McCammon C, Kupenko I et al. (2020) Author Correction: Discovery of Fe7O9: A New Iron Oxide with a Complex Monoclinic Structure. Sci Rep 10(1): 6622.

35. Zhou Z, Yang L, Gao J, Chen X (2019) Structure-Relaxivity Relationships of Magnetic Nanoparticles for Magnetic Resonance Imaging. Adv Mater 31(8): e1804567.

36. Zhang W, Liu L, Chen H, Hu K, Delahunty I et al. (2018) Surface Impact on Nanoparticle-Based Magnetic Resonance Imaging Contrast Agents. Theranostics 8(9): 2521–2548.

37. Phan CM, Nguyen HM (2017) Role of Capping Agent in Wet Synthesis of Nanoparticles. J Phys Chem A 121(17): 3213–3219.

38. Boros E, Gale EM, Caravan P (2015) MR Imaging Probes: Design and Applications. Dalton Trans 44(11): 4804–4818.

39. Peng E, Wang F, Xue JM (2015) Nanostructured Magnetic Nanocomposites as MRI Contrast Agents. J Mater Chem B 3(11): 2241–2276.

40. Li F, Zhi D, Luo Y, Zhang J, Nan X (201) Core/Shell Fe_3O_4/Gd_2O_3 Nanocubes as T1-T2 Dual Modal MRI Contrast Agents. Nanoscale 8(25): 12826–12833.

41. Ni D, Zhang J, Bu W, Zhang C, Yao Z et al. (2016) Gylated $NaHoF_4$ Nanoparticles as Contrast Agents for Both X-Ray Computed Tomography and Ultra-High Field Magnetic Resonance Imaging. Biomaterials 76: 218–225.

42. Pedersen DB, Duncan S (2005) Substituent Effects on the Adsorption of Dialkyl Sulfides on Gold Nanoparticles. J Phys Chem A 109 (49):11172–11179.

43. Rieffel J, Chitgupi U, Lovell JF (2015) Recent Advances in Higher-Order, Multimodal, Biomedical Imaging Agents. Small 11 (35): 4445–4461.

44. Neuwelt EA, Hamilton BE, Varallyay CG, Rooney WR, Edelman RD (2009) Ultrasmall Superparamagnetic Iron Oxides (USPIOs): A Future Alternative Magnetic Resonance (MR) Contrast Agent for Patients at Risk for Nephrogenic Systemic Fibrosis (NSF)?. Kidney Int 75 (5): 465–474.

45. Estelrich J, Sánchez Martín MJ, Busquets MA (2015) Nanoparticles in Magnetic Resonance Imaging: From Simple to Dual Contrast Agents. Int J Nanomedicine 10: 1727–1741.

46. Pysanenko A, Habartová A, Svrčková P, Lengyel J, Poterya V et al. (2015) Lack of Aggregation of Molecules on Ice Nanoparticles. J Phys Chem A 119 (34): 8991–8999.

47. Ling D, Lee N, Hyeon T (2015) Chemical Synthesis and Assembly of Uniformly Sized Iron Oxide Nanoparticles for Medical Applications. Acc Chem Res 48 (5): 1276–1285.

48. Tang Y, Zhang C, Wang J, Lin X, Zhang L et al. (2015) MRI/SPECT/Fluorescent Tri-Modal Probe for Evaluating the Homing and Therapeutic Efficacy of Transplanted Mesenchymal Stem Cells in a Rat Ischemic Stroke Model. Adv Funct Mater 25 (7): 1024–1034.

49. Wiesner HM, Balla DZ, Shajan G, Scheffler K, Uğurbil K et al. (2016) 17O Relaxation Times in the Rat Brain at 16.4T. Magn Reson Med 75 (5): 1886–1893.

50. Roberto García-Figueiras, Sandra Baleato-González, Anwar R. Padhani, Antonio Luna-Alcalá, Juan Antonio Vallejo-Casas et al. (2019) How clinical imaging can assess cancer biology. Insights into Imaging 28(1).

51. Saritas EU, Goodwill PW, Croft LR, Konkle JJ, Lu K et al. (2013) Magnetic Particle Imaging (MPI) for NMR and MRI Researchers. J Magn Reson 229: 116–126.

52. Yin X, Russek SE, Zabow G, Sun F, Mohapatra J et al. (2018) Large T1 Contrast Enhancement Using Superparamagnetic Nanoparticles in Ultra-Low Field MRI. Sci Rep 8(1): 11863.

53. Wyss PP, Lamichhane S, Rauber M, Thomann R, Krämer KW et al. (2016) Tripod USPIONs with High Aspect Ratio Show Enhanced T2 Relaxation and Cytocompatibility. Nanomedicine (Lond) 11(9): 1017–1030.

54. Yang L, Zhou Z, Liu H, Wu C, Zhang H et al. (2015) Europium-Engineered Iron Oxide Nanocubes with High T1 and T2 Contrast Abilities for MRI in Living Subjects. Nanoscale 7(15): 6843–6850.

55. Song XR, Wang X, Yu SX, Cao J, Li SH et al. (2015) Co_9 Se_8 Nanoplates as a New Theranostic Platform for Photoacoustic/Magnetic Resonance Dual-Modal-Imaging-Guided Chemo-Photothermal Combination Therapy. Advanced Materials 27(21): 3285–3291.

56. Mulder WJM, Strijkers GJ, Van Tilborg GAF, Griffioen AW, Nicolay K (2006) Lipid-Based Nanoparticles for Contrast-Enhanced MRI and Molecular Imaging. NMR Biomed 19(1): 142–164.

57. Choi H, Lee YS, Hwang DW, Lee DS (2016) Translational Radio nanomedicine: A Clinical Perspective. European Journal of Nanomedicine 8 (2): 71–84.

58. Jeong HH, Mark AG, Alarcón Correa M, Kim I, Oswald P et al. (2016) Dispersion and Shape Engineered Plasmonic Nanosensors. Nat Commun 7: 11331.

59. Brotton SJ, Kaiser RI (2021) Effects of Nitrogen Dioxide on the Oxidation of Levitated Exo-Tetrahydrodicyclopentadiene (JP-10) Droplets Doped with Aluminum Nanoparticles. J Phys Chem A 125(13): 2727–2742.

60. Upadhyay S, Parekh K, Pandey B (2016) Influence of Crystallite Size on the Magnetic Properties of Fe3O4 Nanoparticles. Journal of Alloys and Compounds 678: 478–485.

61. Vannier MW (2009) CT Clinical Perspective: Challenges and the Impact of Future Technology Developments. Annual International Conference of the IEEE Engineering in Medicine and Biology Society, pp. 1909–1912.

How to cite this article: Homeira F. Physicochemical Transformation Effect on the Relaxivity Enhancement of Iron Oxide Nanoparticles in Biomedical Imaging. Biostat Biom Open Access J. 2023; 11(2): 555810. DOI: 10.19080/BBOAJ.2023.11.555810

62. Catana C, Procissi D, Wu Y, Judenhofer MS, Qi J et al. (2008) Simultaneous in Vivo Positron Emission Tomography and Magnetic Resonance Imaging. Proc Natl Acad Sci USA 105(10): 3705–3710.

63. Ernesto Forte, Dario Fiorenza, Enza Torino, Angela Costagliola di Polidoro, Carlo Cavaliere et al. (2022) Radiolabeled PET/MRI Nanoparticles for Tumor Imaging. Journal of Clinical Medicine 9(1): 89.

64. Bouziotis P, Psimadas D, Tsotakos T, Stamopoulos D, Tsoukalas C (2012) Radiolabeled Iron Oxide Nanoparticles As Dual-Modality SPECT/MRI and PET/MRI Agents. Current Topics in Medicinal Chemistry 12(23): 2694–2702.

65. Chen K, Conti PS (2010) Target-Specific Delivery of Peptide-Based Probes for PET Imaging. Advanced Drug Delivery Reviews 62(11): 1005–1022.

66. De Rosales RTM (2014) Potential Clinical Applications of Bimodal PET-MRI or SPECT-MRI Agents. Journal of Labelled Compounds and Radiopharmaceuticals 57(4): 298–303.

67. Baetke SC, Lammers T, Kiessling F (2015) Applications of Nanoparticles for Diagnosis and Therapy of Cancer. Br J Radiol 88(1054): 20150207.

68. Peer D, Karp JM, Hong S, Farokhzad OC, Margalit R et al. (2007) Nanocarriers as an Emerging Platform for Cancer Therapy. Nature Nanotech 2(12): 751-760.

69. Elvin Blanco, Haifa Shen, Mauro Ferrari (2015) Principles of nanoparticle design for overcoming biological barriers to drug delivery | Nature Biotechnology 33: 941-951.

70. Radeloff K, Ramos Tirado M, Haddad D, Breuer K, Müller J et al. (2021) Superparamagnetic Iron Oxide Particles (VSOPs) Show Genotoxic Effects but No Functional Impact on Human Adipose Tissue-Derived Stromal Cells (ASCs). Materials (Basel) 14(2): 263.

71. Feng Q, Liu Y, Huang J, Chen K, Huang J et al. (2018) Uptake, Distribution, Clearance, and Toxicity of Iron Oxide Nanoparticles with Different Sizes and Coatings. Scientific Reports 8(1): 2082.

72. Stylianopoulos T, Jain RK (2015) Design Considerations for Nanotherapeutics in Oncology. Nanomedicine: Nanotechnology, Biology and Medicine 11(8): 1893-1907.

73. Dallet L, Stanicki D, Voisin P, Miraux S, Ribot EJ (2021) Micron-Sized Iron Oxide Particles for Both MRI Cell Tracking and Magnetic Fluid Hyperthermia Treatment. Scientific Reports 11(1): 3286.

74. Kuo YT, Herlihy AH, So PW, Bhakoo KK, Bell JD (2005) In Vivo Measurements of T1 Relaxation Times in Mouse Brain Associated with Different Modes of Systemic Administration of Manganese Chloride. J Magn Reson Imaging 21(4): 334–339.

75. Jafari A, Salouti M, Shayesteh SF, Heidari Z, Rajabi AB et al. (2015) Synthesis and Characterization of Bombesin-Superparamagnetic Iron Oxide Nanoparticles as a Targeted Contrast Agent for Imaging of Breast Cancer Using MRI. Nanotechnology 26(7): 075101.

76. Xie W, Guo Z, Gao F, Gao Q, Wang D et al. (2018) Shape-, Size- and Structure-Controlled Synthesis and Biocompatibility of Iron Oxide Nanoparticles for Magnetic Theranostics. Theranostics 8(12): 3284–3307.

77. Zhao Z, Zhou Z, Bao J, Wang Z, Hu J et al. (2013) Octapod Iron Oxide Nanoparticles as High-Performance T_2 Contrast Agents for Magnetic Resonance Imaging. Nature communications 4: 2266.

78. Zhao HY, Liu S, He J, Pan CC, Li H et al. (2015) Synthesis and Application of Strawberry-like Fe3O4-Au Nanoparticles as CT-MR Dual-Modality Contrast Agents in Accurate Detection of the Progressive Liver Disease. Biomaterials 51: 194–207.

79. Jiao Mingxia, Jianfeng Zeng, Lihong Jing, Chunyan Liu, Mingyuan Gao et al. (2021) Flow Synthesis of Biocompatible Fe3O4 Nanoparticles: Insight into the Effects of Residence Time, Fluid Velocity, and Tube Reactor Dimension on Particle Size Distribution | Chemistry of Materials 27(4): 1299-1305.

80. Faridnejad H (2022) Design and Simulation of the Source (Wiggler) and Medical Beamline of Iranian Light Source Facility (ILSF) for Medical Applications. Biostatistics and Biometrics Open Access Journal 10(4): 555793.

DOI: 10.19080/BBOAJ.2023.11.555810

How to cite this article: Homeira F. Physicochemical Transformation Effect on the Relaxivity Enhancement of Iron Oxide Nanoparticles in Biomedical Imaging. Biostat Biom Open Access J. 2023; 11(2): 555810. DOI: 10.19080/BBOAJ.2023.11.555810